

## Recovery of two-phase microstructures of planar isotropic elastic composites.

Tomasz Łukasiak

Warsaw University of Technology, Warsaw, Poland, t.lukasiak@il.pw.edu.pl

### 1. Abstract

The isotropic elastic mixtures composed of two isotropic materials of the bulk moduli ( $\kappa^2 > \kappa^1$ ) and shear moduli ( $\mu^2 > \mu^1$ ) are characterized by the effective bulk and shear moduli  $\kappa^*$  and  $\mu^*$ . In the planar problems the theoretically admissible pairs  $(\kappa^*, \mu^*)$ , for given volume fraction  $\rho_0$  of material  $(\kappa^2, \mu^2)$ , lie within a rectangular domain of vertices determined by the Hashin-Shtrikman bounds. The tightest bounds in 2D known up till now are due to Cherkaev and Gibiansky (CG). The microstructures corresponding to the interior of the CG area can be of arbitrary rank, in the meaning of the hierarchical homogenization. In the present paper a family of composites is constructed of the underlying microstructures of rank 1. The consideration is confined to the microstructures possessing rotational symmetry of angle  $120^\circ$ . To find the effective moduli  $(\kappa^*, \mu^*)$  the homogenization method is used: the local basic cell problems are set on a cell  $Y$  of the shape of a hexagonal domain. The periodicity conditions refer to the opposite sides of  $Y$ . Such a non-conventional basic cell choice generates automatically the family of isotropic mixtures. The subsequent points  $(\kappa^*, \mu^*)$  are found by solving the inverse homogenization problems with the isoperimetric condition expressing the amounts of both the materials within the cell. The isotropy conditions, usually explicitly introduced into the inverse homogenization formulation, do not appear, as being fulfilled by the microstructure construction. The method put forward makes it possible to localize each admissible pair  $(\kappa^*, \mu^*)$  by appropriate choice of the layout of both the constituents within the repetitive sub-domain of  $Y$ .

**2. Keywords:** isotropic composites, inverse homogenization, recovery of microstructures.

### 3. Introduction

Knowing all microproperties of the representative volume element (RVE) of a considered composite material one can obtain its effective properties by the direct homogenization method [9]. This can be done by treating RVE as a repetitive cell  $Y$  with accurate approximations under some commonly accepted assumptions of randomness, see [15]. According to the homogenization theory the effective moduli are expressed by the formulae involving solutions to the so-called basic cell problems. The problems can be solved by the Finite Element Method (FEM) [7], [16], preceded by a proper discretization of the RVE identified here with a periodicity cell  $Y$ .

The inverse homogenization means reconstructing the layout of given materials (usually isotropic) within RVE to achieve prescribed effective properties of the composite. This topic is indissolubly bonded with the topology optimization [13] since the optimal designs turn out to possess composite structure with highly complicated local properties of the underlying microstructure [2]. The first approximation of the effective moduli of two-phase composites of materials  $M^{(1)}$  and  $M^{(2)}$  distributed arbitrarily is due to Voigt (of 1889 expressed by the arithmetic mean, VR bounds), the lower bounds are due to Reuss (a harmonic mean, 1929). More accurate estimates for an isotropic composites composed of two well-ordered isotropic materials were specified by Hashin and Shtrikman in 1963 and extended by Walpole in 1966 to the case of non-ordered materials. these bounds are called Hashin-Shtrikman-Walpole bounds (HSW). The tightest bounds CG in 2D known up till now are due to Cherkaev and Gibiansky [3]. The generalization of the CG bounds for the Kirchhoff plates can be found in [5]. The CG bounds are described by a curvilinear rectangle of vertices A, B, C, D, the vertices A and C being Hashin-Shtrikman points, B being attributed to the Walpole result see fig.(1). In the planar problems the theoretically admissible pairs  $(\kappa^*, \mu^*)$ , for given volume fraction  $\rho_0$  of material  $M^{(2)} = (\kappa^2, \mu^2)$ , should lie within a curvilinear rectangular domain determined by Cherkaev and Gibiansky. The challenge is to design a microstructure whose effective properties correspond to the extreme points of the CG bounds. By obtaining such microstructures we verify the theoretical results by Cherkaev and Gibiansky. Such task is a structural topology optimization problem and is known as inverse homogenization regarding to the extreme composites. New extreme composite structures and the proposed new microstructures reaching the CG limits are shown in [10], yet there are some points on the boundaries of the admissible CG area for which the structure is not known until today (e.g. point B). Many optimization techniques have been used to attain the CG bounds, including the Method of Moving Asymptotes (MMA) [14] and Sequential Linear Programming SLP [13] to mention the most promising. Nevertheless, due to numerical properties of the FE method used for homogenisation, the problem is still tough to solve and only approximate solutions can be obtained. The present paper refers to the topology optimization formulation in which invariants of the constitutive tensor, here bulk and shear moduli, are predefined at each point

of the feasible domain [4]. We present a numerical algorithm to reconstruct in RVE the 2D layout of two isotropic materials of given bulk moduli  $\kappa^2 > \kappa^1 > 0$  and shear moduli  $\mu^2 > \mu^1 > 0$  (well-ordered materials) for the corresponding shapes of  $Y$ , i.e. the hexagon for 2D, and its relevant internal topology fig.(2) i.e. rotational symmetry of angle  $120^\circ$ . This algorithm allows to obtain for a fixed ratio  $\rho_0$  of materials amount (isoperimetric condition) such layout with the assumed (admissible) pair  $(\kappa^*, \mu^*)$  representing the effective isotropic properties of the periodic composite. The goal of this work is to find isotropic composites whose parameters  $(\kappa, \mu)$  are as near as possible to, or even reach the Cherkhaev-Gibiansky bounds.

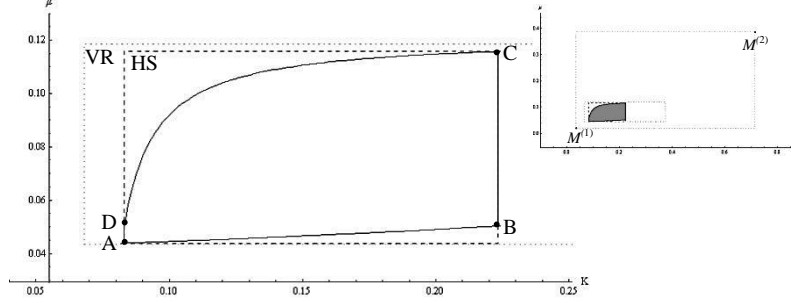


Figure 1: Theoretically admissible  $(\kappa^*, \mu^*)$  for  $M^{(1)}=(5/7, 5/13)/20$ ,  $M^{(2)}=(5/7, 5/13)$ ,  $\rho_0=1/2$ .  
Dotted-VR bounds, Dashed – HS bounds.

#### 4. Numerical homogenization

The algorithm used follows from imposing the FE approximation on the solution to the basic cell problems of the homogenization theory [16]. It can be shortly summarized as follows:

Let periodic  $Y$  be uniformly divided into  $\Omega_k$  elements ( $k=1..m$ ) each element-wise constant material  $\mathbf{E}_k$ , the nodal displacement  $\mathbf{q}$  determine the displacement field  $\mathbf{u} = \mathbf{N}\mathbf{q}$  and the strain field  $\boldsymbol{\varepsilon} = \mathbf{B}\mathbf{q}$  within  $\Omega_k$ , with  $\mathbf{N}$  being shape functions and  $\mathbf{B}$  being the geometric matrix and formally  $\mathbf{B}=\mathbf{D}\mathbf{N}$  where  $\mathbf{D}$  is the matrix of the differential operators for plane stress/strain problem.  $\mathbf{E}_k=\mathbf{E}(\kappa_k, \mu_k)$  describe constitutive matrix of the  $k$ -th element

$$\mathbf{E}(\kappa, \mu) = \begin{bmatrix} \kappa + \mu & \kappa - \mu & 0 \\ \kappa - \mu & \kappa + \mu & 0 \\ 0 & 0 & \mu \end{bmatrix} \quad \mathbf{D} = \begin{bmatrix} \frac{\partial}{\partial x} & 0 & \frac{\partial}{\partial y} \\ 0 & \frac{\partial}{\partial y} & \frac{\partial}{\partial x} \end{bmatrix}^T \quad (1)$$

for plane stress problem

We define for each element  $k$  the matrices

$$\mathbf{H}_e(\mathbf{E}_k) = \mathbf{H}_k = \int_{\Omega_k} \mathbf{E}_k \mathbf{B}_k d\Omega_k$$

$$\mathbf{K}_e(\mathbf{E}_k) = \mathbf{K}_k = \int_{\Omega_k} \mathbf{B}_k^T \mathbf{E}_k \mathbf{B}_k d\Omega_k \quad (2)$$

Due to uniform mesh we have for each element  $\mathbf{B}_k = \mathbf{B}_0$ . Let  $\sum_k^*$  and  $\langle * \rangle = |*|^{-1} \int * dY$  stand for the finite elements aggregations over all elements and the averaging over the  $Y$  respectively. The effective constitutive matrix reads

$$\mathbf{E}^{eff} = \left\langle \sum_k \mathbf{E}_k \right\rangle - \left\langle \sum_k \mathbf{H}_k \right\rangle \left\langle \sum_k \mathbf{K}_k \right\rangle^{-1} \left\langle \sum_k \mathbf{H}_k \right\rangle^T$$

$$\mathbf{E}^{eff} = \mathbf{E}^{avg} - (\mathbf{H}\mathbf{K}^{-1}\mathbf{H}^T) |Y|^{-1} \quad (3)$$

The periodicity condition is fulfilled by the corresponding numbering of nodes at opposite edges with the identical meshing on them. Corresponding nodes have the same numbers i.e. the same degree of freedoms. By a process of aggregation this is automatically taken into account in the construction of global matrices  $\mathbf{K}$  and  $\mathbf{H}$ . The  $\mathbf{H}$  matrix comprises three separate, self-equilibrated load cases. Thus, the three different FEM problems for three column vector  $\mathbf{q}$  are to be solved, namely

$$\mathbf{K}\mathbf{q} = \mathbf{H}^T \quad (4)$$

and finally Eq.(3) can be written as

$$\mathbf{E}^{eff} = \mathbf{E}^{avg} - \mathbf{H}\mathbf{q} |Y|^{-1} \quad (5)$$

Assuming the results within the class of the rank-1 microstructures the layout of the material properties is parameterized by the density function  $\rho \in [0, 1]$  distributed element-wise  $\rho_k$  constant within  $Y$ . At each element  $k$  we assume  $\rho_k$ -dependent isotropic material. One can assume SIMP-like or RAMP-like material approximation with arbitrary chosen ‘‘penalty’’ parameter  $p$  (usually  $p=3$ ).

$$\begin{aligned}\kappa_k^{\text{SIMP}^*}(\rho_k) &= \kappa_k^{\text{SIMP}^*} = (1 - \rho_k^p) \kappa_1 + \rho_k^p \kappa_2, & \mu_k^{\text{SIMP}^*}(\rho_k) &= \mu_k^{\text{SIMP}^*} = (1 - \rho_k^p) \mu_1 + \rho_k^p \mu_2 \\ \kappa_k^{\text{RAMP}^*}(\rho_k) &= \kappa_k^{\text{RAMP}^*} = \frac{(1 - \rho_k) \kappa_1 + \rho_k \kappa_2}{1 + (1 - \rho_k)p}, & \mu_k^{\text{RAMP}^*}(\rho_k) &= \mu_k^{\text{RAMP}^*} = \frac{(1 - \rho_k) \mu_1 + \rho_k \mu_2}{1 + (1 - \rho_k)p}\end{aligned}\quad (6)$$

(Note, that classical SIMP or RAMP involve only on the Young moduli  $E_1, E_2$  while the Poisson ratio  $\nu$  remains unperturbed [1], [8]. Other approximations of the material properties for the intermediate  $\rho$  may also be used [12] and [6].

Prior to solving the optimization problem we construct the formulae for the gradient of  $\mathbf{E}^{\text{eff}}$  with respect to the variables  $\rho_k$ . These derivatives are expressed by

$$\frac{\partial \mathbf{E}^{\text{eff}}}{\partial \rho_k} = \frac{1}{|Y|} f(p, \rho) \left( \mathbf{E}_\Delta A_k - \mathbf{H}_\Delta \mathbf{R} + \mathbf{R}^T \mathbf{K}_\Delta \mathbf{R} - \mathbf{R}^T \mathbf{H}_\Delta^T \right) \quad (7)$$

Where:  $A_k = |\Omega_k|$ ,  $\mathbf{R} = \mathbf{K}^{-1} \mathbf{H}^T$ ,  $\mathbf{H}_\Delta = \mathbf{H}(\mathbf{E}_\Delta)$ ,  $\mathbf{K}_\Delta = \mathbf{K}(\mathbf{E}_\Delta)$ ,  $\Delta \kappa = \kappa_2 - \kappa_1$ ,  $\Delta \mu = \mu_2 - \mu_1$

and for SIMP\*:  $\mathbf{E}_\Delta = \mathbf{E}(\Delta \kappa, \Delta \mu)$ ,  $f(p, \rho) = \rho \rho^{p-1}$

whilst for RAMP\*:  $\mathbf{E}_\Delta = \rho \rho \mathbf{E}(\Delta \kappa, \Delta \mu)$ ,  $f(p, \rho) = \frac{1}{(1 + (1 - \rho)p)^2}$

## 5. Optimization problem for isotropic periodicity

In general, the inverse homogenization problem, which is in fact 01-optimization problem to be solved, is relaxed by allowing intermediate values of  $\rho$ . This relaxation allows the use of the gradient methods. The relaxed problem reads:

(P1)

For some mesh density and initial distribution of  $\rho_k$  for  $Y$  and given desired homogenized parameters

Minimize: the gap between the desired and actual parameters

Subject to: - bounds for design variables

- constrains for volume fraction

- isotropy conditions

The actual homogenized parameters are calculated from some homogenization formula on given distribution of element-wise  $\rho_k$  e.g. Eq.(4). Variables  $\rho_k$  are changed according to the gradient of the objective function and constraints, and the process is repeated until the material is distributed sufficiently close to the exact 01-solution (i.e. for each element  $\rho_k \equiv 0$ , or  $\rho_k \equiv 1$ ). Due to nonlinearity respect to  $\rho_k$  (i.e.  $\mathbf{H} = \mathbf{H}(\rho_k)$ ,  $\mathbf{K} = \mathbf{K}(\rho_k)$  see Eq.(3b)) many local minima occur so the direct application of the gradient method is problematic. This can be partially avoided by additional penalty component incorporated to the objective function forcing the 01-solution. The proper material approximation for intermediate values plays also important role. The parameter  $p$  in Eq.(6), often called as ‘‘penalization parameter’’, aims to penalize the intermediate value of variables. Moreover one can apply some filtering techniques to avoid or rather escaping from the local minima. These can be used for filtering  $\rho_k$  or to filtering the components of the gradient [11]. These methods are controlled by many parameters, the nature of which is not entirely clear. Despite the simplifications and tricks used the obtained results are still relatively far from the CG bounds.

One way to obtain more accurate results is a simplification of the optimization by decreasing number of constraints (reformulate the problem to the convex one is rather impossible). This can be achieved by a suitable choice the shape of the  $Y$  (i.e. the periodicity) and its internal structure. The hexagonal repetitive cell with internal rotational symmetry of 120 degree gives strictly isotropic homogenized constitutive matrix for 2D linear elasticity homogenization problem. It is known from theory of the 4<sup>th</sup> rank tensors. For 2<sup>nd</sup> rank tensors in 2D (governing e.g. thermal problems) the isotropy is realized by the square repetitive cell with internal rotational symmetry of 180 degree. So the last constraint(s) in (P1) relating to the ‘‘isotropic conditions’’ may be omitted. What’s more, the use of hexagonal cells significantly reduces the number of variables. Due to its internal symmetry only one-third the entire cell elements is treated as independent variables  $\rho_k$ . Finally, a rectangular cell usually used to obtain the isotropic properties is far greater than hexagonal one, and requires a much larger number of the finite elements to achieve the same level of accuracy, see fig.(3).

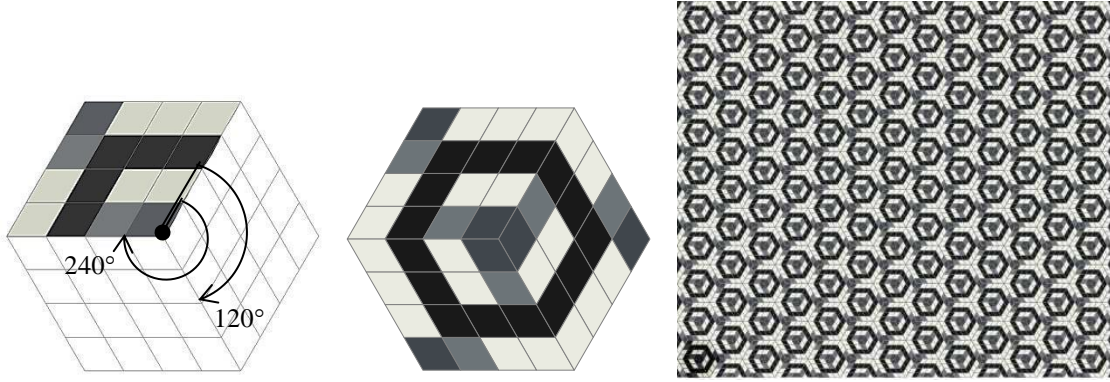


Figure 2: Topology of the hexagon isotropic cell.

It should be noted that the selection of a periodic cell shape greatly affects the quality of the results obtained in terms of isotropy conditions. In the problems of the homogenization of the isotropic tensor of the 4-th rank, the solution of the problem for a square-shaped cell, even when if the cell is divided to a very large number of elements, will never fulfils conditions of isotropy exactly. Thus solution of the (PI) for a square-shaped cell of periodicity is not possible. It is possible to fulfil the conditions of isotropy on a cells of rectangular but only for rectangles of the right dimensions ratio. Of course there are many other shapes of cells of periodic for which can be attained the condition of the isotropy, for example some groups of adjacent hexagonal cells. But, the hexagonal cell is the smallest of the possible shapes of the cells realizing the structures of a periodic for the constitutive isotropic tensor the 4-th rank and requires the least number of elements, so the problem (PI) contain the smallest number of the decision variables. The smallest for two-materials a isotropic structure is realized on a cell of rhomb shaped of which is divided along shortest diagonal into two triangles and each of the isotropic materials occupy its own triangle and therefore as such is rather useless for a practical use.

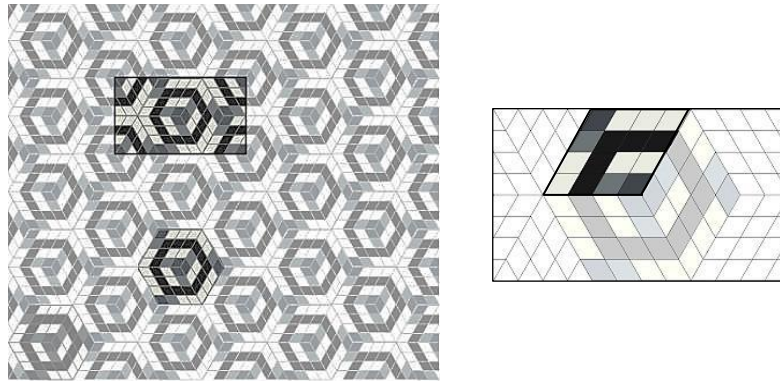


Figure 3: Comparing the sizes of the hexagon and the rectangular cell of periodicity.

The last technical improvement of the presented algorithm is due to the nature of the load matrix  $\mathbf{H}$  imposed on the cell in the process of homogenization Eq.(4). Non-zero loads i.e. matrix components, are generated only on the nodes located on the interface of materials thus nodes lying within the area of each material are “unnecessary”, see fig. (4). This fact is exploited by applying superelements. It mimics the “virtual” dense mesh in each element (its subdivision) but without any internal nodes in it. This allows for increased accuracy by applying a higher degree of elements i.e. higher degree of the shape functions. Thus the common dimensions of the matrices  $\mathbf{K}$  and  $\mathbf{H}$  are slightly reduced. In the case of a six node triangular element the number of Degrees Of Freedoms (DOF) is reduced by about 20% for “virtual” subdivision into 4 sub-elements and at least 35% for subdivision into 9 sub-elements, see fig.(5). Given that the cost of solving the system of linear equations is proportional to  $n^3$  ( $n$  is the number of DOFs) savings are respectively about 50% and 80% of the time needed to solve Eq.(4) and calculating Eq.(7) in case of standard dense mesh. It should be noted, however, that then the time needed for calculating the matrices  $\mathbf{K}_k$  increases. The calculation of each of them requires solving a system of linear  $n_h$  equations ( $n_h$  is the number of internal DOFs which in the superelement are eliminated). Leaving aside the question of saving time, it should be noted that the use of superelements clearly increases the accuracy of the results of numerical homogenization process. Consequently, the calculated components of the gradient of the objective function are more precise.

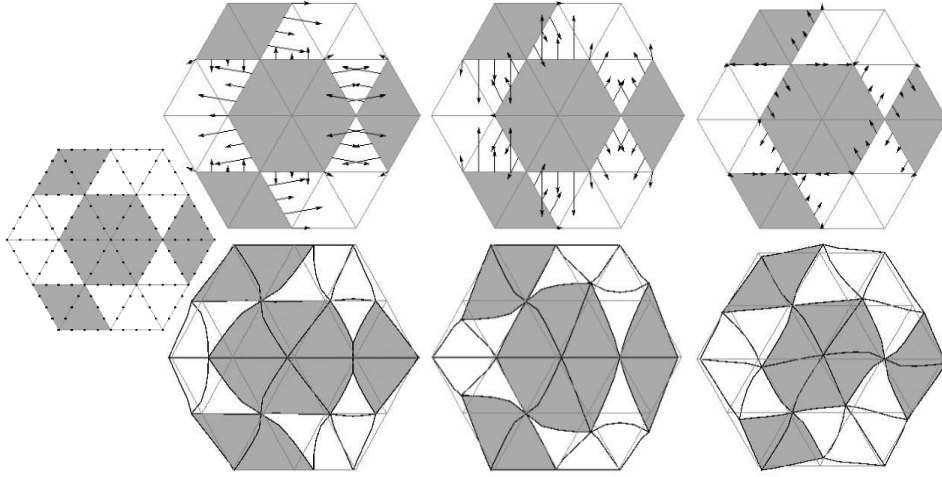


Figure 4: Visualization of the structure of the matrix  $\mathbf{H}$ . The periodic displacements.

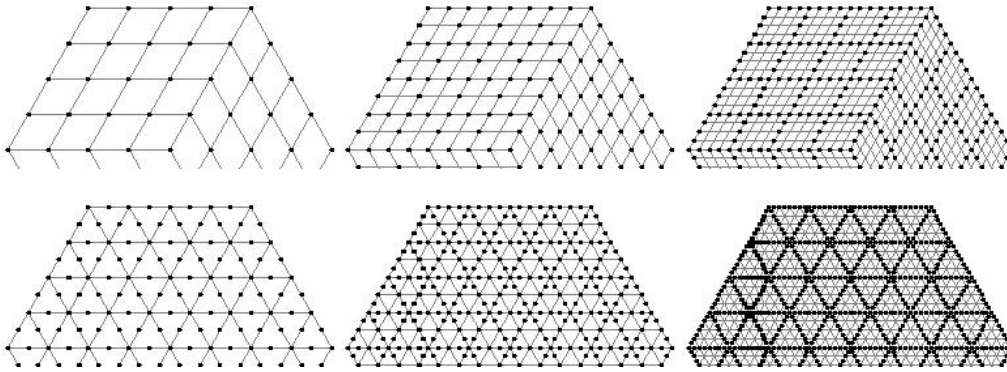


Figure 5: Nodes of the superelements: for 4-nodes four edge element and for 6-nodes triangular element

The objective function for the discussed inverse problem and  $\boldsymbol{\rho} = \{\rho_k\}$  is chosen as below:

$$P(\boldsymbol{\rho}) = \left( \frac{\kappa^* - \kappa}{\kappa^*} \right)^2 + \left( \frac{\mu^* - \mu}{\mu^*} \right)^2 + w_{01} \sum_k \rho_k (1 - \rho_k) \quad (8)$$

The optimization problem assumes the form

for given  $(\kappa^*, \mu^*)$  and  $\rho_0$  find :

$$\min_{\rho_k} P(\boldsymbol{\rho})$$

subject to:

$$0 \leq \rho_k \leq 1 \quad k = 1 \dots m$$

$$\frac{1}{m} \sum_k \rho_k = \rho_0 \quad (\text{the isoperimetric condition})$$

(9)

In Eq.(8) the pair  $(\kappa, \mu)$  is calculated from the homogenized constitutive matrix for the data values of  $\boldsymbol{\rho}$ , namely  $\mathbf{E}^{eff} = \mathbf{E}(\kappa, \mu)$ . Hereafter in this article this interpretation of the pair  $(\kappa, \mu)$  will be kept.

Due to the shape and the topology of the periodicity cell  $Y$  no penalty terms are needed to enforce isotropic results. The only, weighted by its own scalar coefficient  $w_{01}$  penalty term aims to speed up the convergence to 01-solution in each element (i.e.  $\rho_k=0$  or  $\rho_k=1$ ). It can be omitted by the adoption of a modified gradient method. This modification forces the 01-solution in some elements selected according to the gradient at each steps of the optimization process. Such 01-solutions must be maintained for those elements till the process stops.

The gradient of the objective function  $\nabla P(\boldsymbol{\rho}) = \{\nabla_k\}$  is calculated from

$$\nabla_k = -2 \left( \frac{1}{(\boldsymbol{\kappa}^*)^2} (\boldsymbol{\kappa}^* - \boldsymbol{\kappa}) \frac{\partial \boldsymbol{\kappa}}{\partial \rho_k} + \frac{1}{(\boldsymbol{\mu}^*)^2} (\boldsymbol{\mu}^* - \boldsymbol{\mu}) \frac{\partial \boldsymbol{\mu}}{\partial \rho_k} \right) + w_{01} (1 - 2\rho_k) \quad (10)$$

where  $\frac{\partial \boldsymbol{\kappa}}{\partial \rho_k} = \frac{1}{2} \left( \frac{\partial \mathbf{E}_{11}^{eff}}{\partial \rho_k} + \frac{\partial \mathbf{E}_{12}^{eff}}{\partial \rho_k} \right)$ ,  $\frac{\partial \boldsymbol{\mu}}{\partial \rho_k} = \frac{1}{2} \left( \frac{\partial \mathbf{E}_{11}^{eff}}{\partial \rho_k} - \frac{\partial \mathbf{E}_{12}^{eff}}{\partial \rho_k} \right)$

To solve Eq.(9) the SLP method is used. It is assumed that the solution to the problem can be achieved by a sequence of solutions to the problems of linear. Expanding the objective function at the point  $\boldsymbol{\rho}$  in a Taylor series and taking into account only the linear members we develop

$$P(\boldsymbol{\rho} + \Delta) = P(\boldsymbol{\rho}) + \sum_k \nabla_k \Delta_k \quad (11)$$

Such local linearization of Eq.(8) allows finding approximated minimum of problem (9) near to point  $\boldsymbol{\rho}$  by solving the following linear problem:

for given  $\{\nabla_k\}$  find :

$$\min_{\Delta \rho_k} \sum_k \nabla_k \Delta \rho_k$$

subject to:

$$\max(0, \rho_k - d) \leq \rho_k + \Delta \rho_k \leq \min(\rho_k + d, 1) \quad k = 1 \dots m$$

$$\sum_k \Delta \rho_k = 0 \quad (\text{the isoperimetric condition})$$

where arbitrarily chosen scalar parameter  $d$  specifies the maximum allowable changes in the values of variables  $\rho_k$  also limited by the 01 bounds. The latter constraint is assumed that the point  $\boldsymbol{\rho}$  satisfies the isoperimetric condition hence the sum of the changes  $\Delta \rho_k$  of the variables  $\rho_k$  has to be zero. This assumption does not affect the process of solution to the problem (9). Just is enough to select the appropriate starting vector  $\{\rho_k\}$  satisfying this condition, but this is trivial. After the solution of (12) the new point  $\boldsymbol{\rho}^{new} = \{\rho_k + \Delta \rho_k\}$  is calculated and then the value of the objective function  $P(\boldsymbol{\rho}^{new})$  is examined. If  $P(\boldsymbol{\rho}^{new}) < P(\boldsymbol{\rho})$  then the values  $\{\rho_k\}$  are updated and for  $\boldsymbol{\rho} \leftarrow \boldsymbol{\rho}^{new}$  the process repeats otherwise it stops and the point  $\boldsymbol{\rho}$  can be regarded as a local minimum of the problem (9) with respect to the fixed distance  $d$ .

## 6. Algorithm

At the starting point  $\boldsymbol{\rho}$  the distribution of the  $\rho_k$  is randomly selected, yet satisfying isoperimetric condition in problem (9). Material approximation model is used to calculate  $\mathbf{K}_k$  and  $\mathbf{H}_k$ . according to Eq.(6). Other models of approximation of the material can also be used. The homogenization process starts, see Eq.(5), and then components of the gradient  $\nabla_k$  of the objective function are calculated according to Eq.(7) and Eq.(10). Next, the local linear optimization problem (12) is solved sequentially with updating the elements of the gradient  $\nabla_k$  and  $\boldsymbol{\rho}$  at each step. If the process stops at a local minimum then the new starting point  $\boldsymbol{\rho}^f$  is selected, namely.

$$\boldsymbol{\rho}^f = \Phi(\boldsymbol{\rho}) \quad (13)$$

The function  $\Phi$  is generally a function of the filtering of the  $\{\rho_k\}$ . In this paper, to set a new starting point a simple volume preserving diluting filter for  $\boldsymbol{\rho}$  is used. New  $\boldsymbol{\rho}$  values are calculated from the formula

$$\rho_k^f = \frac{\sum_n w_n \rho_n}{\sum_n w_n} \quad n \in N_k \quad (14)$$

where set  $N_k$  contain a collection of elements of the neighboring to the element  $k$  and himself. It's a simple, familiar with operations on bitmap images, graphics filter. The weight values  $w_i$  are shown in fig.(6). The effect of this filtering is a blurring of the  $\rho_k$  values in the elements that are at the interface of materials. Filtering takes into account the periodicity of the cell by momentarily its extension to the adjacent elements. More complex methods of morphological filtering  $\boldsymbol{\rho}$  and the gradient of the objective function are described in [11]. The optimization process (12) is further continued with the  $\boldsymbol{\rho}^f$ . However, this approach does not guarantee a 01-solution to the problem even if the  $w_{01} > 0$ , see Eq.(8). In the presented examples it is assumed that  $w_{01}=0$ , and a different technique to force the 01 solutions is used. The obtained 01-solution for some of the elements at previous steps of (12) during the subsequent steps is preserved till the end of the process. They can be only modified by filtering

process (13) in case of stop in local minimum. This method allows to speed up the optimization process because the components of the gradient for these elements need not be calculated. Calculating the gradients  $\nabla_k$  is most time consuming part of the inverse homogenization process.

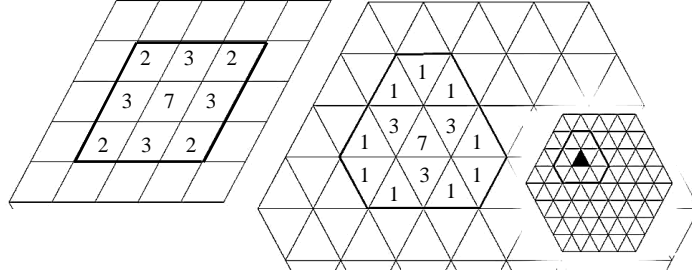


Figure 6: Filtering of the variables  $\rho_k$ . Weights for quadrangle and triangle elements of the mesh.

It is well known that for the nonconvex nonlinear optimization problems, even tackled by the well-tuned approximation method, the final result depends strongly upon the choice of the starting point. So the several optimization processes should be executed, each for different starting point. This, of course, does not guarantee finding the global solution but only suboptimal one and is time-costly. To reduce the computation time we have adopted the following “*adaptive*” computation system:

the process departs from a coarse mesh  $h^{(1)}$  for a randomly assumed vector  $\mathbf{p}^{(1)}$ . Upon obtaining the 01-solutions or even to achieve a local minimum for this mesh, we make it denser, creating the mesh of smaller  $h^{(2)}$ . For this mesh we define a new vector  $\mathbf{p}^{(2)}$  such that  $\langle \mathbf{p}^{(1)} \rangle = \langle \mathbf{p}^{(2)} \rangle$ . Practically, the structure of the material placement described by  $h^{(1)}$  is covered by new mesh  $h^{(2)}$  and for such covering the new value  $\mathbf{p}^{(2)}$  are calculated see. fig.(7). This step can be completed by one or more pass filtering (13) and becomes a departure point for the next optimization process.

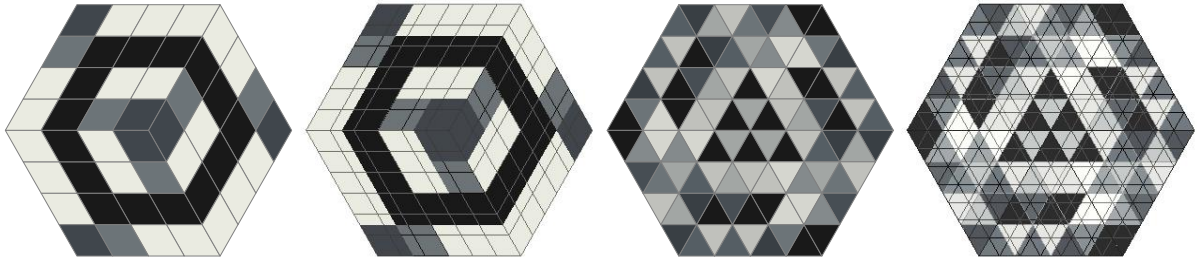


Figure 7: Creating a new 6-layers (for quad) and 7-layers (for triangle) meshes for next step of the optimization.

The proposed “*adaptive*” routine helps to overcome the problems with stopping the optimization process at a local minimum. Furthermore, in the first steps of optimization, for the coarse mesh, can be found the exact solution to the problem with using a binary optimization method, so for dense mesh the next step starts from point which is as close as possible from the optimal solution considering to the mesh size. The time needed to solve the problem in “*adaptive*” manner and to reach the desired mesh density  $h$  is almost the same as in case of the solution for the problem for the adopted starting point with the size of the mesh of  $h$ . For the final mesh consisting of 5400 twelve-nodes elements (three combined 6-nodes triangle elements ie. in total 1800 decision variables, 54 000 DOF) solution time was approximately 1-2 hours on desktop computer (Intel i7 3.6 GHz processor, 16GB RAM).

## 7. Results

The structure of the representative cells and the corresponding composite structures recovered by this process for triangular 12-nodes superelements (4 x 6-nodes elements) are shown. For all the presented cases adopted  $(\kappa_1, \mu_1) = (5/7, 5/13)/20$ ,  $(\kappa_2, \mu_2) = (5/7, 5/13)$  and  $\rho_0 = 0.5$ . Material for the  $\rho_k$  was approximated as SIMP\* with  $p=3$ . For a given objective function (8) the coefficient  $w_{01}=0.0$  is assumed. For all the presented results were the same fixed starting point, i.e.  $\mathbf{p} = \mathbf{p}^{start}$ ,  $\dim(\mathbf{p}^{start}) = 18$ ,  $\langle \mathbf{p}^{start} \rangle = \rho_0$  and  $0.4 < \rho_k^{start} < 0.6$ . Sequential solution (12) was carried out for initial  $d = 0.1$ . This value was reduced to zero iteratively of  $\Delta d = 0.01$  when the value of the objective function at the point  $\mathbf{p}^{new}$  was greater than for  $\mathbf{p}$ . For final  $\mathbf{p}$  was done single pass filtering (14). Then sequential solution (12) was repeated until the convergence of the local minimum, or to obtain a 01-solution. Then the denser mesh was created and process repeats.

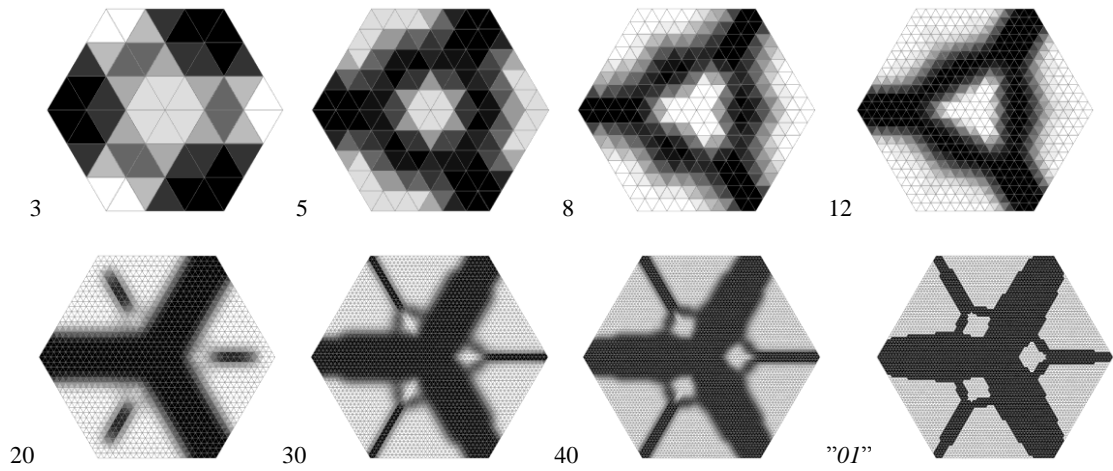


Figure 8: Final results on each “adaptive” step of inverse homogenization process and approximated 01-solution. Number of layers  $L$  are shown. (numbers of elements =  $3 (2 L^2)$ )

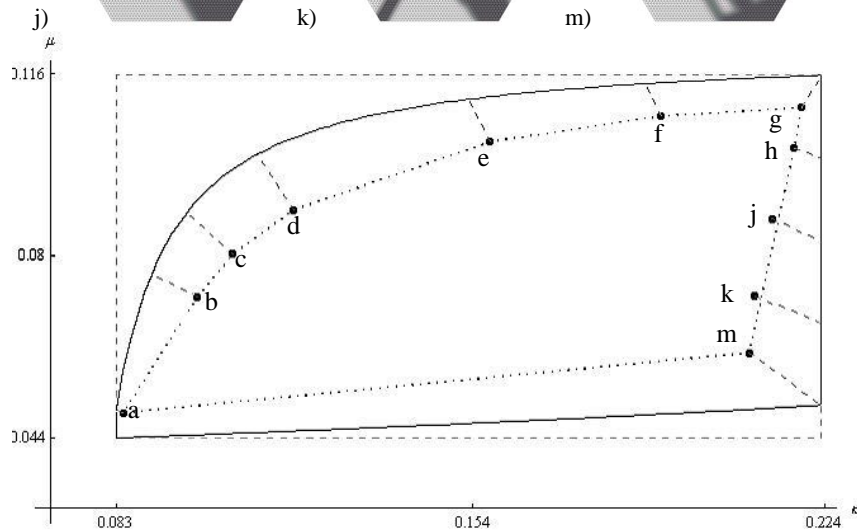
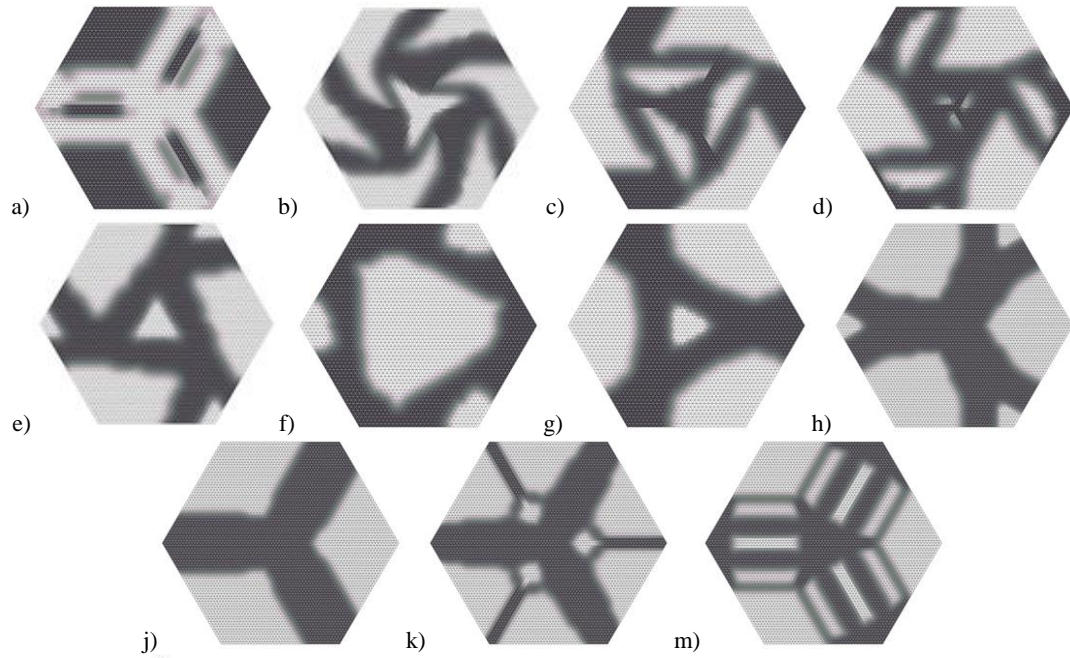
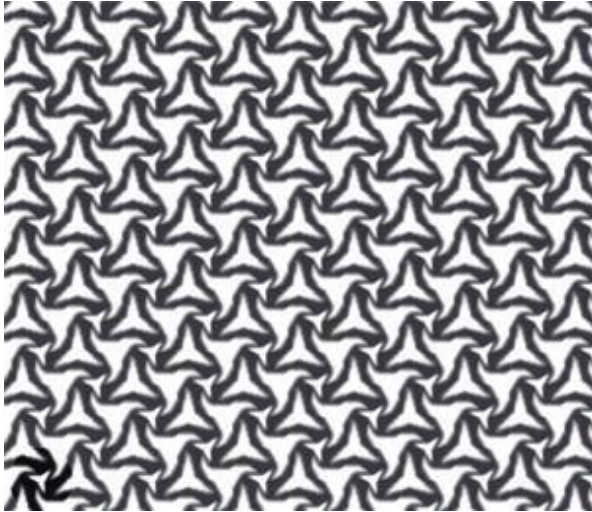


Figure 9: Selected points  $(\kappa, \mu)$  within the CG domain (a..m) and the underlying microstructures. The dashed lines show the assumed  $(\kappa^*, \mu^*)$ . The mesh size: for (a..f)  $L=30$ , for (g..m)  $L=40$ .





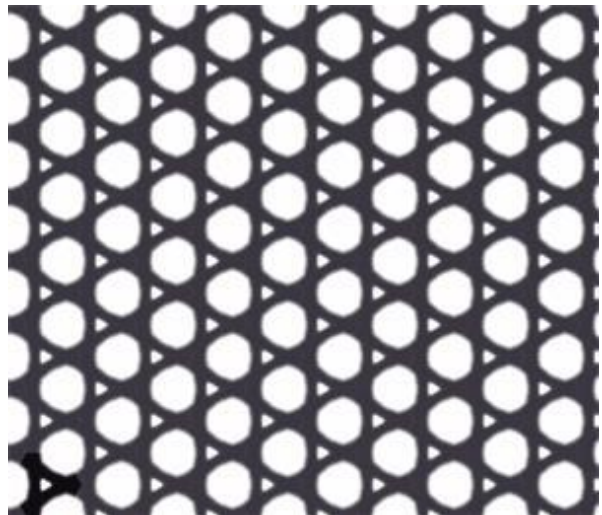
**b)**  $(\kappa, \mu) = (0.099, 0.072)$ ,  $(\kappa^*, \mu^*) = (0.090, 0.076)$



**c)**  $(\kappa, \mu) = (0.106, 0.80)$ ,  $(\kappa^*, \mu^*) = (0.097, 0.089)$



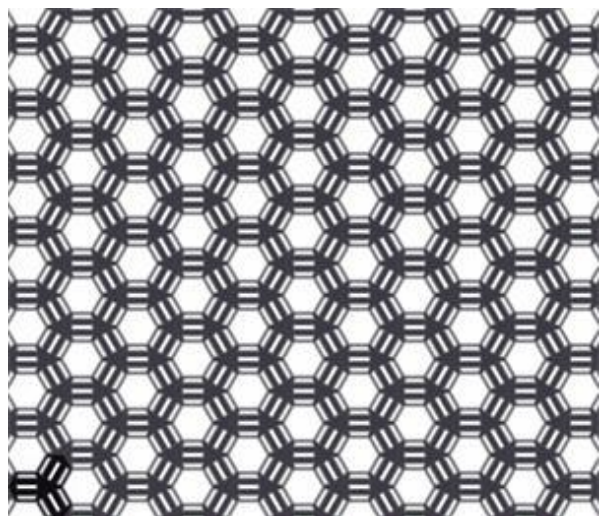
**e)**  $(\kappa, \mu) = (0.157, 0.103)$ ,  $(\kappa^*, \mu^*) = (0.153, 0.111)$



**g)**  $(\kappa, \mu) = (0.219, 0.109)$ ,  $(\kappa^*, \mu^*) = (0.224, 0.116)$



**k)**  $(\kappa, \mu) = (0.210, 0.072)$ ,  $(\kappa^*, \mu^*) = (0.223, 0.067)$



**m)**  $(\kappa, \mu) = (0.209, 9.608)$ ,  $(\kappa^*, \mu^*) = (0.224, 0.061)$

Figure 10: Images of the isotropic composites for selected results.

## 8. Final remarks

The present paper put forward a new algorithm of the numerical inverse homogenization for the planar isotropic composites. The paper is aimed at finding the rank-1 subclass of the isotropic composites of effective moduli achieving the Cherkhaev-Gibiansky (CG) bounds. The key point of this algorithm is the use of the hexagonal cell of periodicity instead of periodicity with a rectangular cell. It is assumed that the internal structure of the hexagonal cell possesses rotational symmetry of angle 120. This assumption results in a significant reduction in the number of design variables to the optimization problem considered (approximately 6 times less than for the case of the cell of a rectangular shape). Moreover, such a cell shape (and its internal symmetry) ensures isotropy of any periodic composites of such class thus essentially reducing the number of constraints involved in the optimization problem. The optimization problem considered has been solved by the SLP method augmented with appropriate filters. It is worth emphasizing that the results obtained lie fairly close to the assumed ones located on the CG bound, but the bounds are not attained. Our results show that the points along the CG bound are attainable only within the class of microstructures of the rank higher than 1. The question: “how big the G-closure for one length-scale isotropic composites is ? “ has been partly answered, but the complete answer remains as an open problem.

## 9. Acknowledgements

The paper was prepared within the Research Grant no N506 071338, financed by the Polish Ministry of Science and Higher Education, entitled: *Topology Optimization of Engineering Structures. Simultaneous shaping and local material properties determination.*

## 10. References

- [1] M.P., Bendsøe, Optimal shape design as a material distribution problem, *Structural Optimization*, 1, 193-202, 1989.
- [2] M.P. Bendsøe and O. Sigmund, *Topology Optimization, Theory, Methods and Application.*, Springer, Berlin, 2003.
- [3] A.V. Cherkhaev and L.V. Gibiansky, Coupled estimates for the bulk and shear moduli of a two dimensional isotropic elastic composite, *Journal of the Mechanics and Physics of Solids*, 41, 937-980, 1993.
- [4] S. Czarnecki and T. Lewiński and T. Łukasiak T., Free material optimum design of plates of pre-defined Kelvin moduli, *World Congress on Structural and Multidisciplinary Optimization*, pp. 13-17, Shizuoka 2011.
- [5] G. Dzierżanowski, Bounds on the effective isotropic moduli of thin elastic composite plates, *Archives of Mechanics*, 62, 253-281, 2010.
- [6] G. Dzierżanowski: On the comparison of material interpolation schemes and optimal composite properties in plane shape optimization, *Structural and Multidisciplinary Optimization*, 46, 693-710, 2012
- [7] B. Hassani and E. Hinton, A review of homogenization and topology optimization, Part I, II, III, *Computers and Structures*, 69, 701–756, 1998.
- [8] G.I.N. Rozvany Aims, scope, methods, history and unified terminology of computer-aided topology optimization in structural mechanics, *Structural and Multidisciplinary Optimization* , 21, 90-108, , 2001.
- [9] E. Sanchez-Palencia, Non-homogeneous media and vibration theory. *Lecture Note in Physics* 127, Springer Verlag, Berlin 1980.
- [10] O. Sigmund, A new class of extremal composites, *Journal of the Mechanics and Physics of Solids*, 48, 397-428, 2000.
- [11] O. Sigmund, Morphology-based black and white filters for topology optimization, *Structural and Multidisciplinary Optimization*, 33, 401-424, 2007.
- [12] O. Sigmund, Material interpolation schemes in topology optimization, *Archive of Applied Mechanics* 69, 635-654, 1999.
- [13] O Sigmund. and S Torquato, Design of smart composite materials using topology optimization, *Smart Materials and Structures*, 8, 365–379, 1999.
- [14] K. Svanberg The method of moving asymptotes—a new method for structural optimization. *International Journal for Numerical Methods in Engineering*, 24, 359–373, 1987.
- [15] S. Torquato, *Random Heterogeneous Materials: Microstructure and Macroscopic Properties.* New York: Springer-Verlag, 2002.
- [16] Woźniak Cz. Nonstandard analysis in mechanics, *Advances in Mechanics*, 1, 3-36, 1986.